

## Research on the anti-corrosion performance of organosilane modified Basalt scales epoxy coating by EIS and SECM

Zhao-zhan Hou<sup>1,#</sup>, Qing-xian Yue<sup>2,#</sup>, Jing Lv<sup>2</sup>, Yu-yu Wang<sup>2</sup>, Bing-qian Zhu<sup>2</sup>, Xuan Liang<sup>2</sup>, Rui Ding<sup>2,\*</sup>, Hai-bin Yu<sup>3</sup>, Xiao Wang<sup>4,5</sup>, Tai-jiang Gui<sup>4</sup>

<sup>1</sup>CRRC Qingdao Sifang Rolling Stock Research Institute Co., LTD., Qingdao 266031, China

<sup>2</sup>College of Oceanology, Yantai University, Yantai, 264005, China;

<sup>3</sup>Key Laboratory of Marine Materials and Related Technologies, CAS, Zhejiang Key Laboratory of Marine Materials and Protective Technologies, Ningbo Institute of Materials Technologies and Engineering, CAS, Ningbo 315201, China;

<sup>4</sup>Marine Chemical Research Institute, State Key Laboratory of Marine Coatings, Qingdao 266071, China;

<sup>5</sup>Ocean University of China, Qingdao 266071, China;

# These authors contributed equally to this work.

\*E-mail: [dingrui@ytu.edu.cn](mailto:dingrui@ytu.edu.cn)

Received: 23 November 2021 / Accepted: 27 December 2021 / Published: 2 February 2022

---

As the new type of natural material, Basalt scales (BS) exhibited flaky micron-sized structure. Due to the acid and alkali resistance and stable chemical properties, it was suitable to act as the filler for anti-corrosion coatings. However, BS showed unsatisfactory compatibility with epoxy resins, and its application was limited. This paper combined the basalt scales with the organosilane by covalent grafting, and prepared organosilane modified basalt scales. The modification of organosilane promoted the combination of basalt scales and epoxy resin and the stability of BS in the coatings by covalent bonds, simultaneously improved the anti-corrosion performance of the coatings. Electrochemical impedance spectroscopy (EIS) experiments showed that organosilane significantly improved the anti-corrosion performance of Basalt scales epoxy coatings, especially the organosilane containing amino groups. The promoting effect of organosilane on the stable dispersion of BS was evaluated by the barrier ability of the coatings to corrosive solutions, and the diffusion dynamics analysis implied the existence of the promoting effect. The enhancement of shielding anticorrosion was result of the optimized dispersion and stability of modified basalt scales.

---

**Keywords:** Basalt scales, Anti-corrosion, Shielding protection kinetics, Coatings

### 1. INTRODUCTION

Anti-corrosion coatings acted as the most commonly used simple and fast technical means for metal corrosion protection [1]. Developing new coatings which showed excellent anti-corrosion ability

was the important content in the field of anti-corrosion technology [2]. Basalt was the natural ore with rich reserves on the earth. Calcium rich clinopyroxene and basic plagioclase were the main mineral components, and the secondary mineral components were olivine, orthopyroxene, iron titanium oxide, quartz and so on [3]. Basalt scales (BS) were the new type of micron flake materials with natural basalt ore as raw material. It was specially processed by screening basalt ore with excellent natural performance, high-temperature melting, clarification, homogenization molding and screening. Compared with other sheet fillers of coatings, basalt scales possessed the wide range of raw materials and low cost. They were resource-saving and environment-friendly materials. Basalt scales showed excellent resistance to medium permeability. Compared with glass flakes, the proportion of iron oxides and aluminum oxides in basalt scales is higher, while there were less alkaline substances [4]. Therefore, basalt scales exhibited stronger acid and alkali resistance than glass flake [5]. Basalt materials would be the worth-trying anti-corrosion fillers due to its geometry, high strength and chemical inertia [6]. However, the interfacial combination between basalt scales and resin should to be raised. The lack of stability would cause microcracks in the coatings and led to the infiltration of corrosive solutions.

In this experiment, basalt scales were modified by organosilane in order to improve the compatibility with epoxy coatings and the satisfactory dispersion of BS. The effect of modification on the anti-corrosion effect of BS epoxy coatings was studied by EIS and scanning electrochemical microscope.

## 2. EXPERIMENTAL METHODS

All chemicals were provided by Aladdin Co., Ltd (China) and analytically pure. Basalt scales (BS) were prepared from natural basalt through special processes such as high-temperature melting and homogenization molding, and implemented by Huazheng Kexin New Material Technology Co., Ltd (China). The micro morphology of the prepared basalt scales was shown in Figure 1, and the basalt scales were less than 10 microns in size. In the ethanol/water (mass ratio 9:1) solution, stirring was continued for 3 hours, and the silane coupling agents KH550 (3-aminopropyl triethoxysilane) or KH560 (3-(2,3-epoxy propoxy) propyltrimethoxysilane) was modified on the basalt scales. Then, by centrifugation treatment and subsequent drying under 45°C, silane coupling agents modified basalt scales were obtained. Blended 1.5g silane coupling agents modified BS (or pure BS) with 10.0 g epoxy curing agents. Continuous mixing operation to ensured that the two were fully mixed. It was then fully mixed with 10.0 g of epoxy polymer to obtain the coatings. Q235 steel electrodes were chosen as the base materials, and its surface was coated by the prepared coatings. The electrode samples were placed in the 50°C drying oven for 2 days.

The electrochemical experiments were implemented on the PAR 2273 electrochemical workstation (Princeton, USA). The saturated calomel electrode acted as the reference electrode. The auxiliary electrode was platinum sheet electrode. The electrochemical experiments were implemented in 3.5 wt% NaCl solutions. In test of EIS, alternating voltage with amplitude of 10 mV and frequency range of 10 mHz~10<sup>5</sup> Hz was applied to the electrode samples. The scan rate of polarization curve measurements was set at 0.333mV/s. The current maps were scanned by scanning electrochemical

microscope (SECM, Sensolytics, Germany) [7]. Three electrode structure was used in the experiments. The working electrode was a platinum ultramicro electrode (UME) with a diameter of 25  $\mu\text{m}$ . The auxiliary electrode was pure platinum. The reference electrode was Ag/AgCl/KCl (3 mol/L) electrode, and all SECM potentials were referenced according to this electrode. The potential of working electrode and substrate was controlled by PGSTAT 302N Metrohm AutoLab bipotentiostat (Utrecht, Netherlands). The UME with an average diameter of 0.05  $\mu\text{m}$  was polished with  $\gamma\text{-Al}_2\text{O}_3$  powder. After ultrasonic degreasing in ethanol and acetone, it was dried in nitrogen. All SECM measurements were performed in a mixed solution of 1 mmol/L ferrocenyl-methanol and 0.1 mol/L KCl by applying a constant potential of -200 mV. This ensured that the oxidation reaction of species at probe tip was controlled by diffusion. The distance from the probe tip to the substrate was controlled to be 15  $\mu\text{m}$ , and the two-dimensional relative motion between the probe and the substrate surface was carried out.

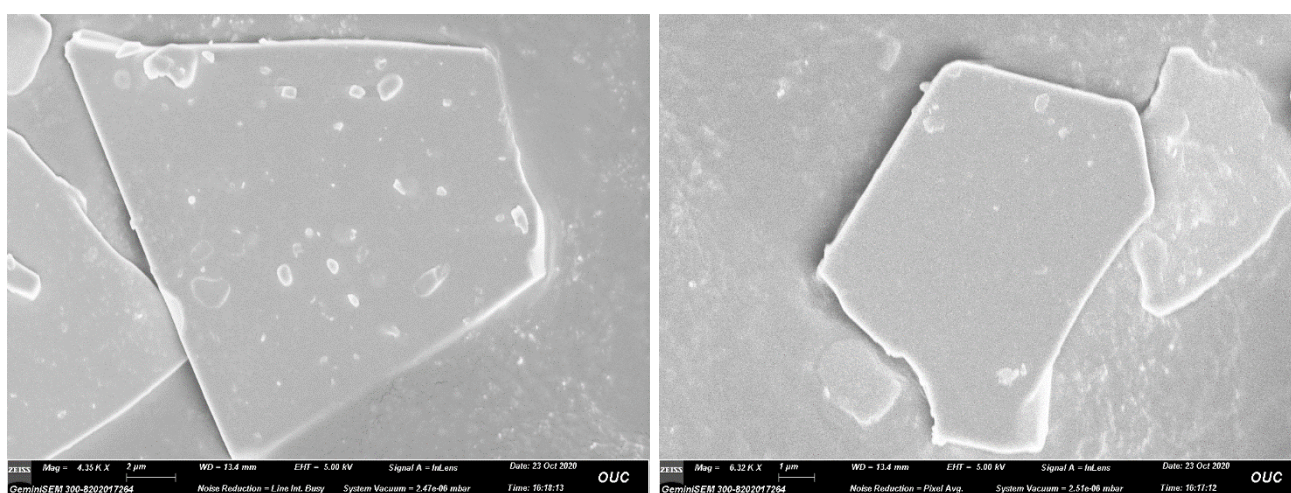


**Figure 1.** The micro morphology of the prepared basalt scales taken by SEM.

### 3. RESULTS AND DISCUSSION

#### 3.1 Global anti-corrosion performance

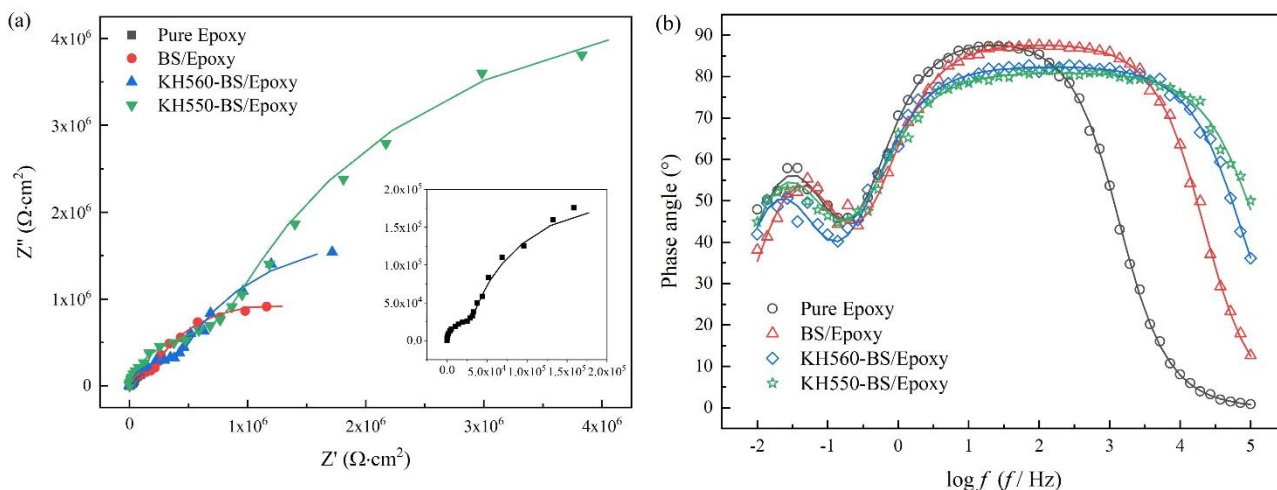
The influence of filler types on the anti-corrosion effect of the coatings was studied by EIS. The EIS of four kinds of epoxy coatings was showed in Figure 2. The difference between coatings was the types of fillers. All samples were immersed in 3.5 wt% NaCl solutions for 24 hours. The improvement of the global impedance of the coatings by various fillers could be derived from the increased capacitive reactance arcs (Figure 2(a)) and low-frequency impedance (Figure 2(c) and (d)). The improvement law of coatings' anti-corrosion effect by various fillers was KH550-BS/Epoxy > KH560-BS/Epoxy > BS/Epoxy > Pure Epoxy. Flake and chemically stable BS improved the barrier ability of the coatings to corrosive media and were conducive to anti-corrosion. The surface improvement of basalt by organosilane ulteriorly promoted the anti-corrosion behaviour of the coatings. The silane coupling agent KH550 showed better performance than KH560. Compared with pure epoxy coatings, the impedance of BS epoxy coatings was improved by about one order of magnitude, which was consistent with Yan's research [8]. The shape information of EIS was provided by Nyquist (Figure 2(a)) and phase angle

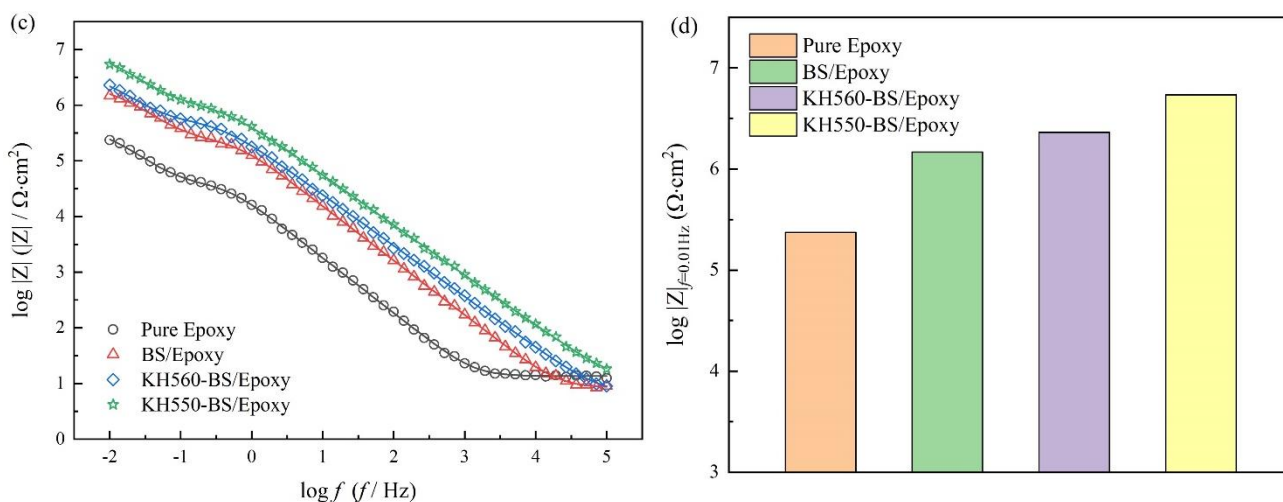
(Figure 2(b)) [9]. The two capacitive reactance arcs in Figure 2(a) and two phase-angle peaks in Figure 2(b) illustrated that the two electrode processes. They were electrochemical corrosion of steel and coatings' dielectric process [10].

According to the distinguishing features of EIS and the actual structural characteristics of coating/steel samples, the Equivalent Circuit B in Figure 3 was chosen to fit the EIS data [11]. Where,  $R_s$  was solution resistance.  $R_c$  was coating resistance.  $R_c$  gave expression to the resistance of the solid phase substance of the coatings which were not completely penetrated by the solution. When the coatings were completely penetrated by the solution,  $R_c$  was the microporous resistance of the coatings. Here,  $R_c$  represented the difficulty of corrosive medium entering the micropores of the coating [12].  $R_{ct}$  was charge transfer resistance. It represented the resistance of the redox reaction of the steel surface.  $Q$  was the constant phase angle element. Its impedance was expressed as

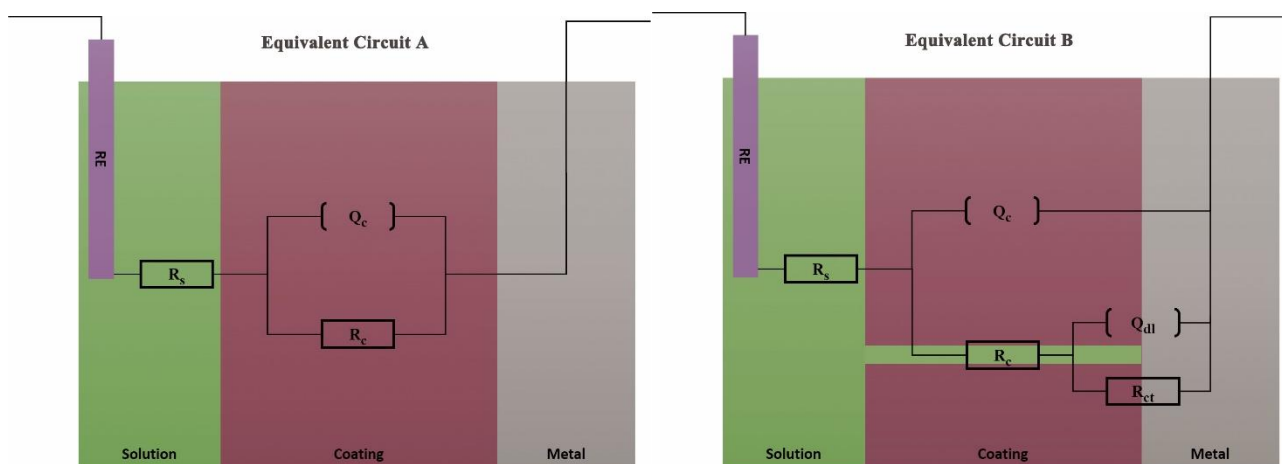
$$Z_Q = \frac{1}{Y_0} \cdot (j\omega)^{-n} \quad (1)$$

Where  $Y_0$  was admittance coefficient. The dispersion coefficient  $n$  reflected the degree to which the actual capacitance deviated from the ideal capacitance [13]. Therefore,  $Q$  was often used to simulate the actual capacitance.  $Q_c$  was the coating capacitance.  $Q_{dl}$  was electric double layer capacitance. Figure 4 displayed the fitting data which explained the influence of fillers on the anti-corrosion effect of the coating in detail. Firstly, the raised values of  $Y_{0,Q_c}$  in Figure 4(a) and dropped  $R_c$  in Figure 4(b) implied the elevated dielectric of the coatings. Secondly, the decrease of  $Y_{0,dl}$  of Figure 4(c) and elevated  $R_{ct}$  in Figure 4(d) signified the contraction of electrochemical active region and the increase of electrochemical reaction resistance. KH550-BS was the most obvious improvement on the corrosion protection effect of the coatings. The reason was that the chemical stable chemical properties and shielding of BS and the improvement of compatibility between BS and epoxy resin by organosilane and optimized dispersion of BS. As shown in Figure 5, epoxy groups of KH560 showed good compatibility with epoxy resins that were also rich in epoxy groups, so it could improve the dispersion of basalt scales. Amino groups in KH550 undergonged a ring-opening reaction with the epoxy groups of epoxy resin, anchoring the Basalt scales to the polymer chain of epoxy resin by means of covalent bonds, so that the Basalt scales were stably dispersed. Obviously, the effect of covalent bond was stronger, and KH550 performed more noticeably than KH560.

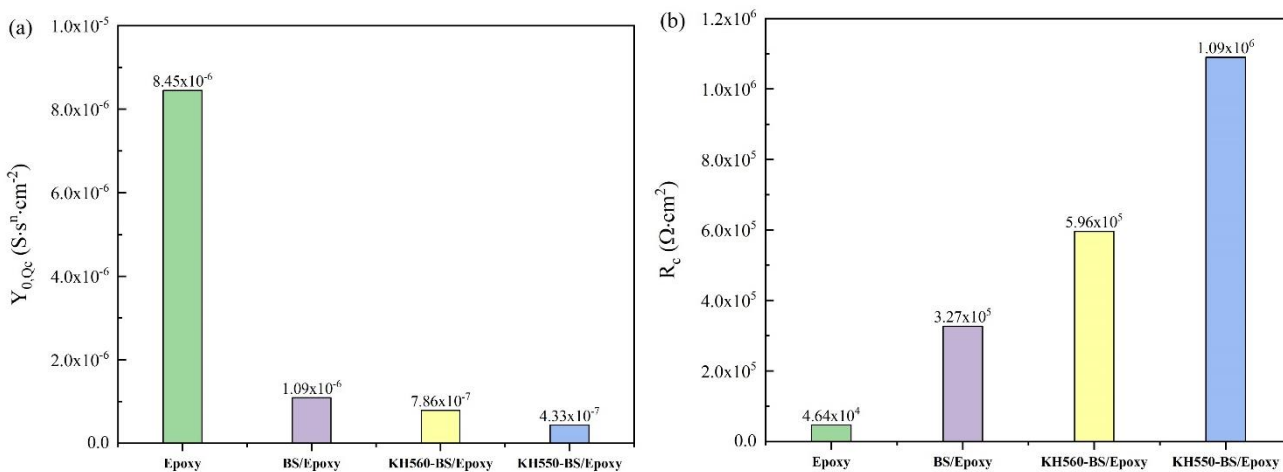




**Figure 2.** Electrochemical impedance spectra of the four coatings immersed in 3.5 wt% NaCl for 24 hours, (a) Nyquist, (b) Bode-phase angle, (c) Bode-impedance modulus  $\log|Z|$ , (d)  $\log|Z|_{f=0.01\text{Hz}}$ .



**Figure 3.** The equivalent circuit established for the fitting of EIS.



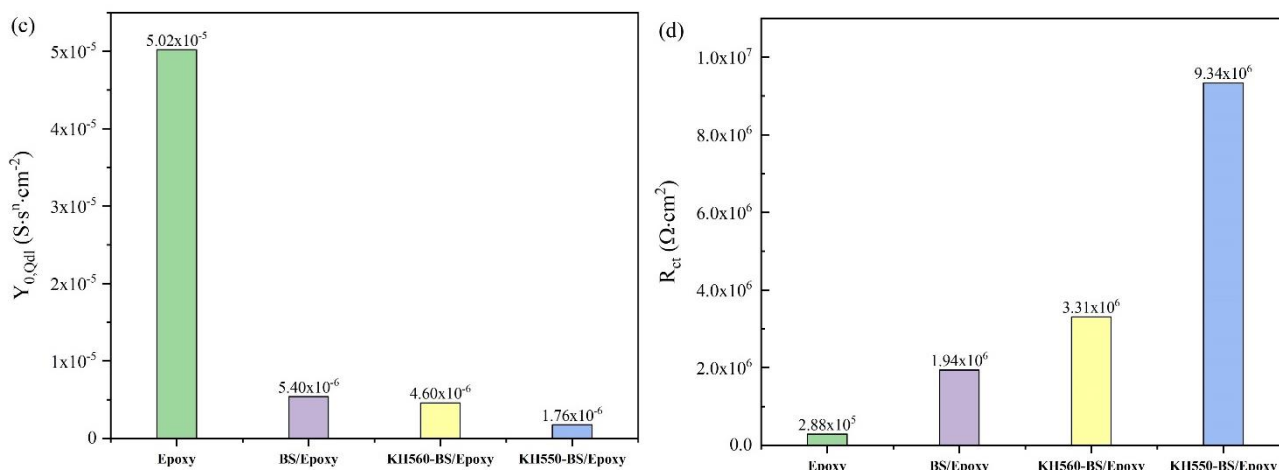
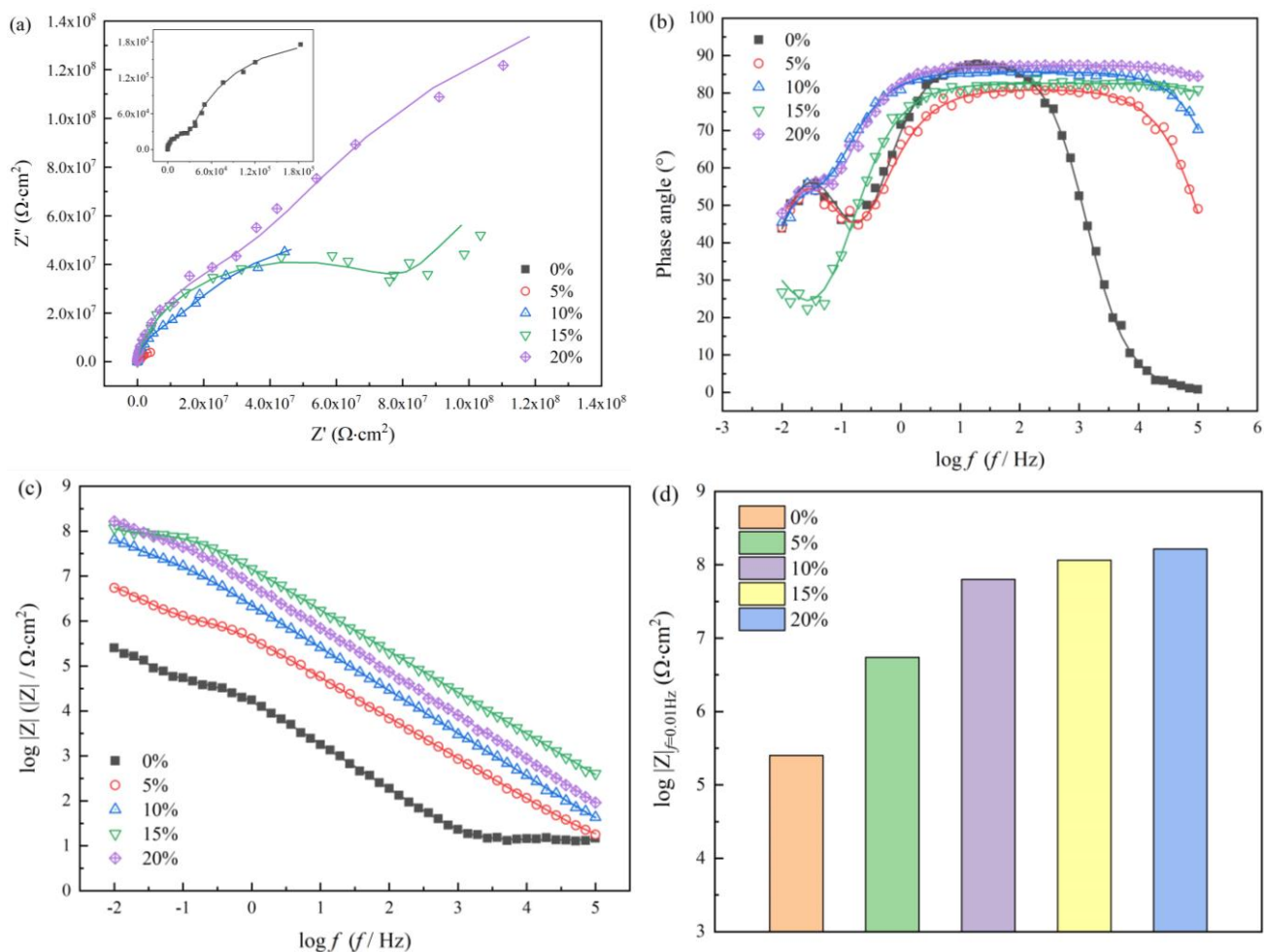


**Figure 4.** The element parameters of (a) coating capacitance, (b) coating resistance, (c) electric double-layer capacitance and (d) charge transfer resistance obtained by the equivalent circuit fitting of EIS of the four kinds of coatings immersed in 3.5 wt% NaCl for 24 hours.

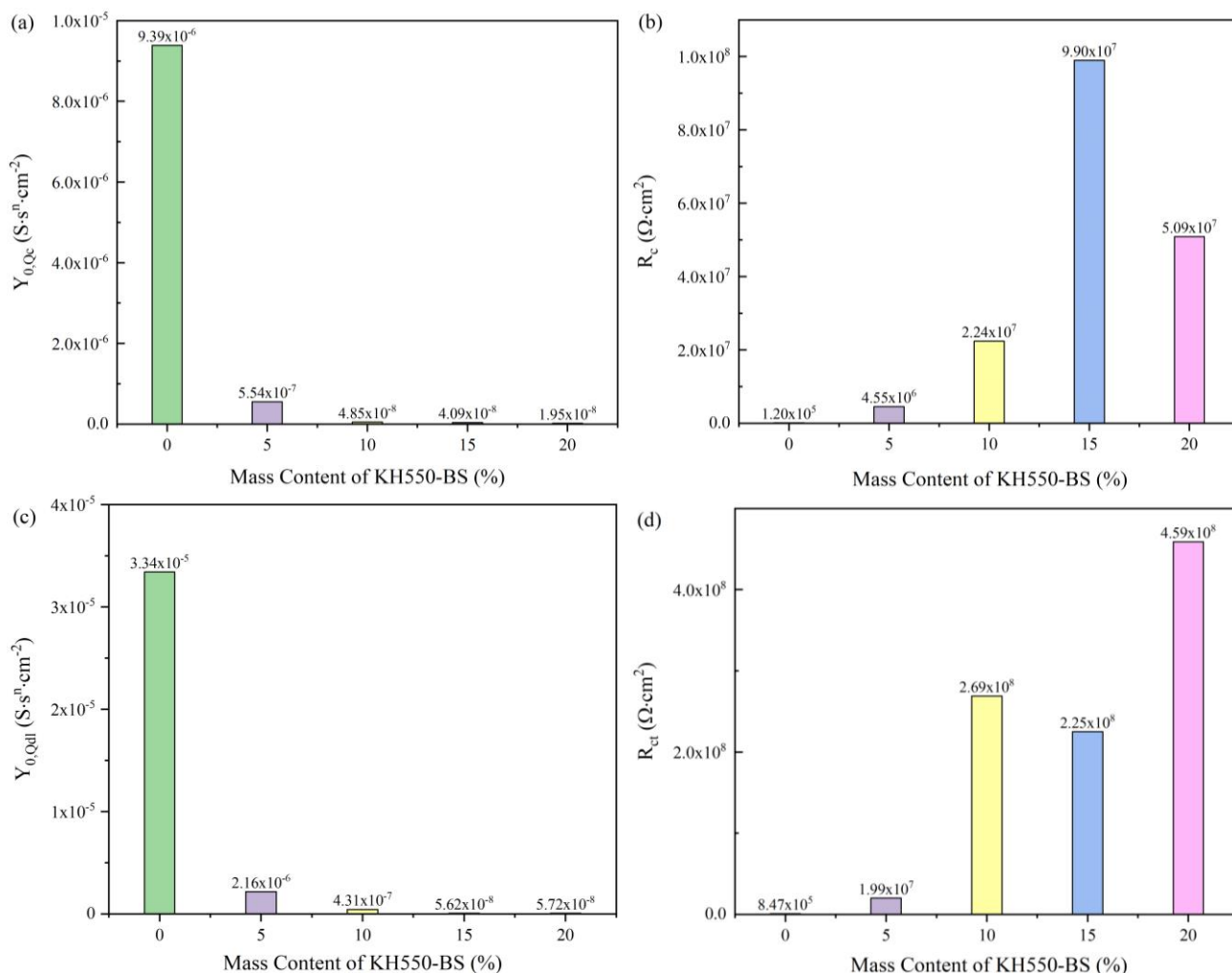
Since the performance of KH550-BS/epoxy coatings was the most significant, the optimal ratio of KH550-BS was investigated. Figure 6 displayed the EIS of the coatings with varied contents of KH550-BS immersed in 3.5 wt% NaCl for 24 hours. The improvement of the global impedance of the coatings by raised mass content of KH550-BS could be derived from the increased capacitive reactance arcs (Figure 6(a)) and low-frequency impedance (Figure 6(c) and (d)). When the content of KH550-BS was greater than 10 wt%, the growth trend of the improvement slowed down. The two capacitive reactance arcs in Figure 6(a) and two phase-angle peaks in Figure 6(b) illustrated that the two electrode processes. They were electrochemical corrosion of steel and coatings' dielectric process. Equivalent Circuit B in Figure 3 was still applicable. The fitting data were shown in Figure 7. The raised values of  $Y_{0,Qc}$  in Figure 7(a) and dropped  $R_c$  in Figure 7(b) implied the elevated dielectric of the coatings. The decrease of  $Y_{0,dll}$  of Figure 7(c) and elevated  $R_{ct}$  in Figure 7(d) signified the contraction of electrochemical active region and the increase of electrochemical reaction resistance. They synergistically proved the mechanism of KH550-BS to lifted the anti-corrosion level of the coatings. The optimal content of KH550-BS was more than 10 wt%. In He's research, the optimal content of polyaniline-modified basalt flakes (PMB) was 10 wt%, which was consistent with our research [14]. Electrochemical impedance spectroscopy showed that the improvement of anti-corrosion performance of the coatings by PMB was mainly manifested in the later stage, and the impedance values of the coatings with or without PMB in the early stage of immersion were similar. The KH550-BS coatings prepared in this experiment showed improvement of 2.5 orders of magnitude in  $|Z|_{f=0.01Hz}$  after being immersed for 24 hours. The best content of basalt flake epoxy coating obtained by Gai through ball milling technology was 15 wt% [15]. Compared with the blank sample, the anti-corrosion performance of the coatings were improved by 2.5 orders of magnitude.



**Figure 5.** The mechanism of two organosilanes improving the dispersion of Basalt scales in epoxy resin.

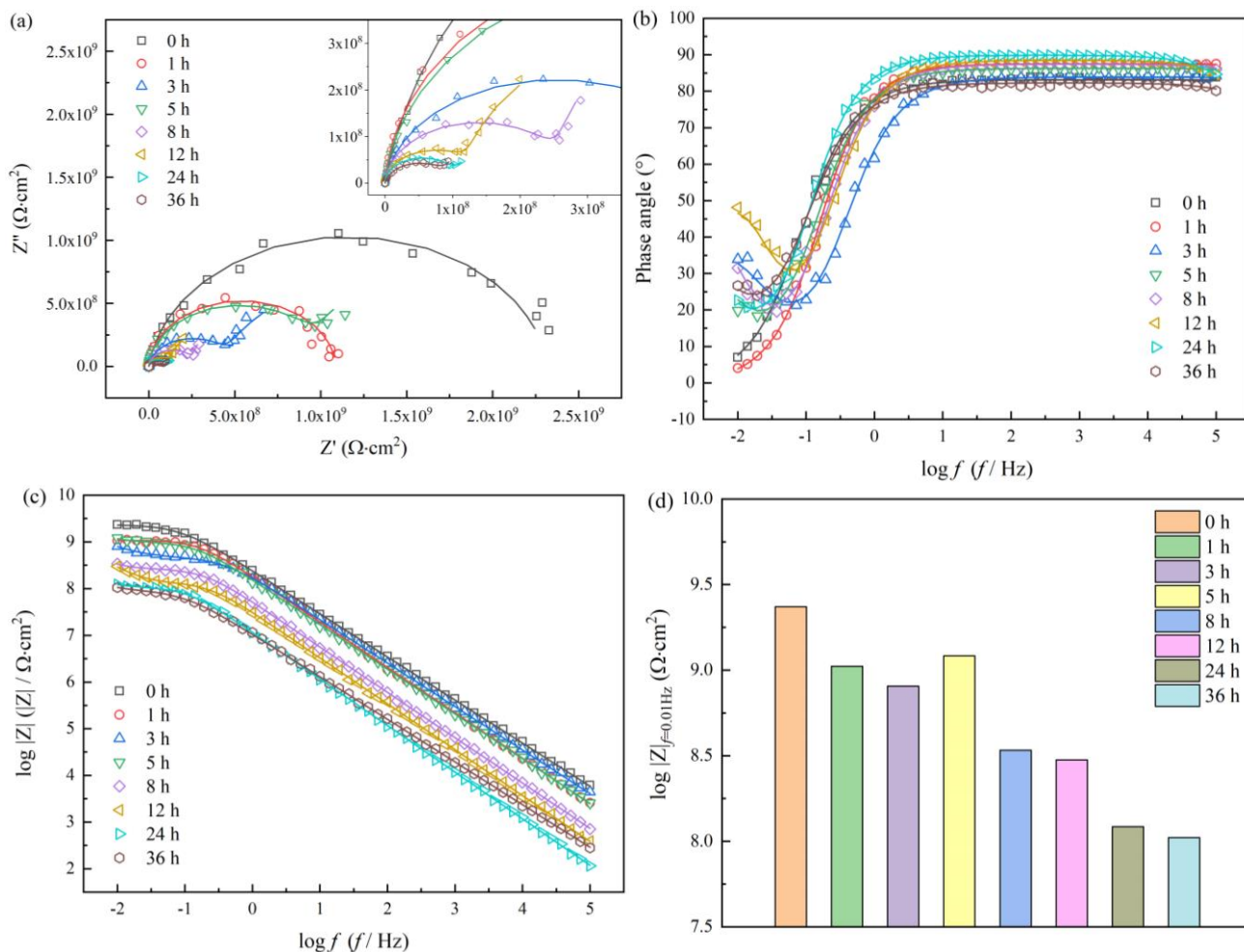


**Figure 6.** Electrochemical impedance spectra of the coatings contained varied contents of KH550-BS immersed in 3.5 wt% NaCl for 24 hours, (a) Nyquist, (b) Bode-phase angle, (c) Bode-impedance modulus  $\log|Z|$ , (d)  $\log|Z|_{f=0.01\text{Hz}}$ .



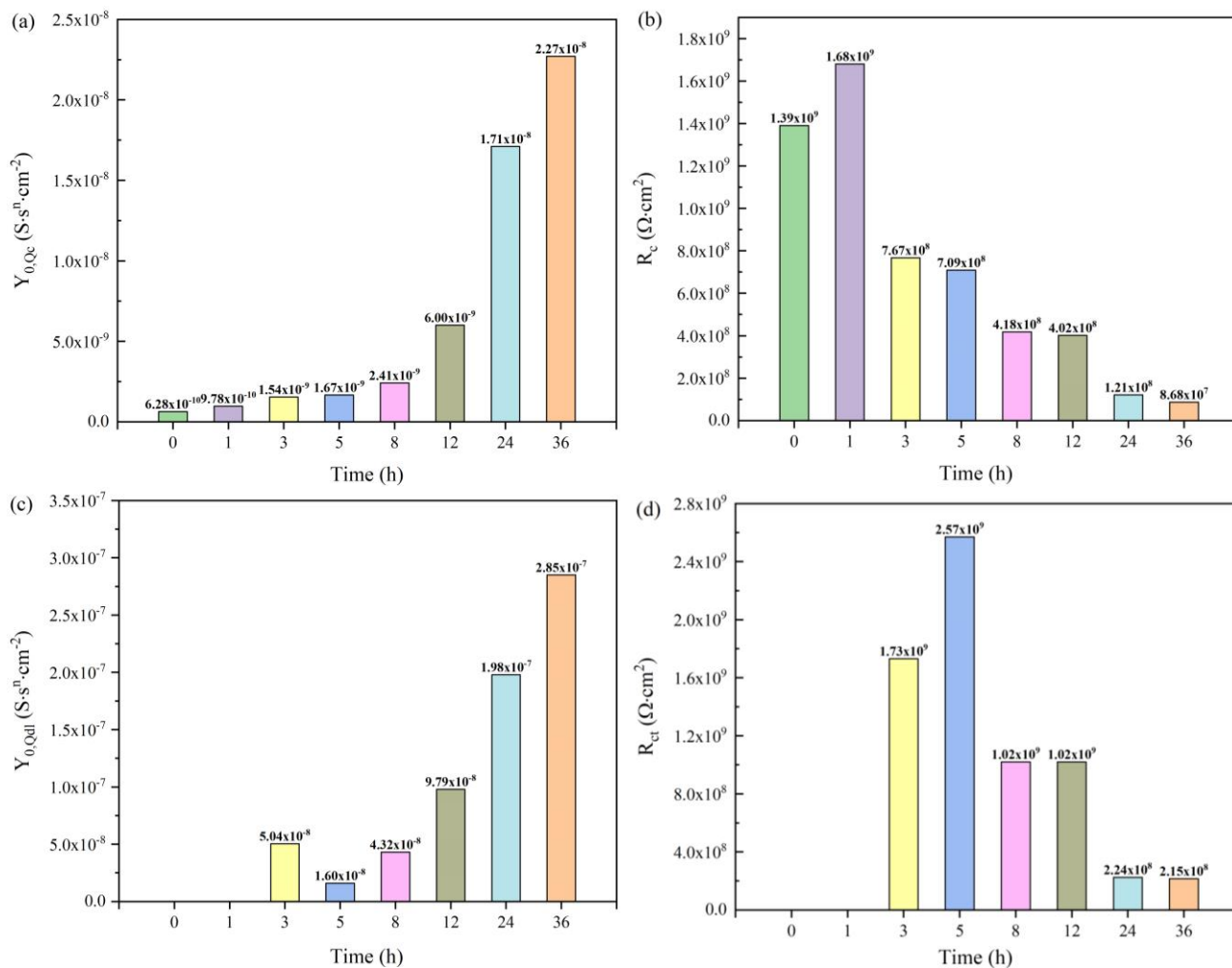
**Figure 7.** The element parameters of (a) coating capacitance, (b) coating resistance, (c) electric double-layer capacitance and (d) charge transfer resistance obtained from fitted EIS of the coatings contained varied contents of KH550-BS immersed in 3.5 wt% NaCl for 24 hours.

Considering the cost performance, the KH550-BS content of 15 wt% was applied for further research. Figure 8 displayed the EIS of the coatings with 15 wt% KH550-BS immersed in 3.5 wt% NaCl for different time. With the penetration of corrosive medium and the development of corrosion reaction, the curvature of capacitive reactance arcs in Nyquist (Figure 8(a)) increased and low frequency impedance modulus in Bode figure ( $\log|Z|_{f=0.01Hz}$ ) (Figure 8(c) and (d)) decreased. In the initial stage (0 hour and 1 hour), the Nyquist diagram (Figure 8(a)) presented one capacitive reactance arc, corresponding to one peak of the Bode-phase angle diagram (Figure 8(b)). This illustrated that in the initial stage, the electrolyte solution did not completely penetrate the coatings, and the electrochemical reaction did not occur. There were one electrode processes, i.e. the coatings' dielectric process, and Equivalent Circuit A (Figure 3) was chosen. When the electrolyte solution completely penetrated the coating (after 3 hours), the second electrode process (electrochemical reaction) began, and the electrochemical impedance spectra reflected the second time constant, which was embodied in the double capacitive reactance arc of Nyquist and the double peak of Bode-phase angle. In this case, equivalent circuit B was still selected.

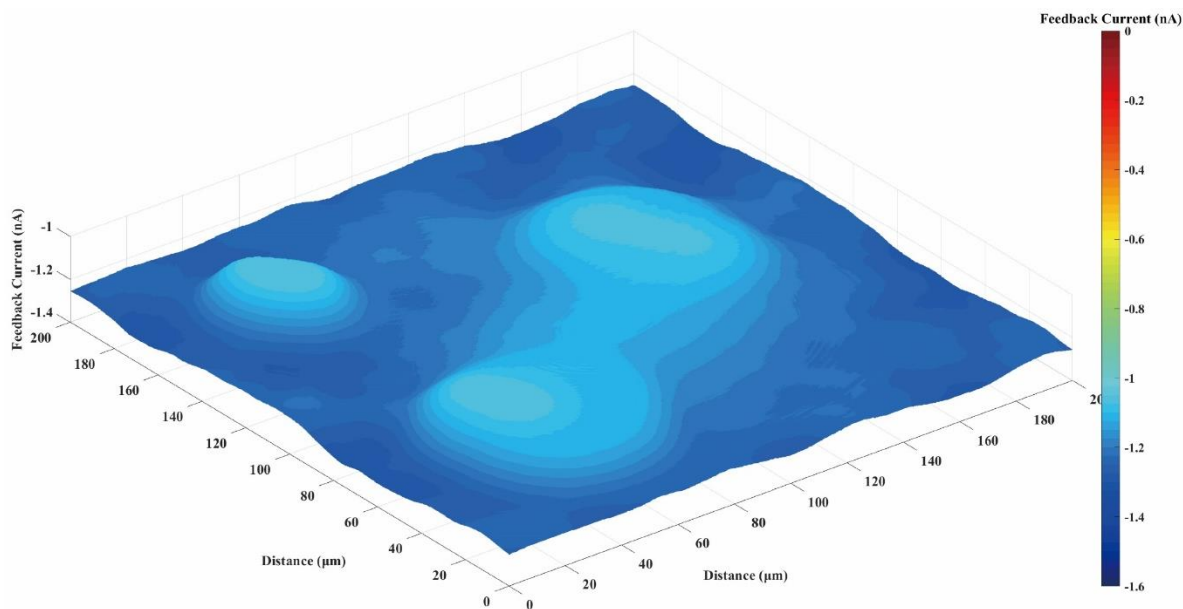


**Figure 8.** Electrochemical impedance spectra of the coatings with 15 wt% KH550-BS after immersion in 3.5 wt% NaCl solution for different time, (a) Nyquist, (b) Bode-phase angle, (c) Bode-impedance modulus  $\log|Z|$ , (d)  $\log|Z|_{f=0.01\text{Hz}}$ .

The fitting data were displayed in Figure 9. With the penetration of corrosive medium and development of corrosion reaction, the dielectric features of the coatings weakened (increase in  $Y_{0,Qc}$  and decrease in  $R_c$ , Figure 9(a) and (b)), the electrochemical active region expanded (increase in  $Y_{0,d1}$ , Figure 9(c)), and electrochemical reaction resistance dropped (decrease in  $R_{ct}$ , Figure 9(d)), which all reflected the gradual deterioration of the coatings. The results of scanning electrochemical microscope (SECM) showed that the degradation process of the coating was uneven. Firstly, the anodic activity was reflected in the scattered local areas (such as impurities or mechanical damage) where the protective performance of the coating was relatively weak. With the development of corrosion, the dispersed anode active regions gradually expanded and were connected as the whole. There was also competition between these anode active regions. For example, the leftmost anode active region in Figure 10 disappeared in the later competition with adjacent anode active regions.



**Figure 9.** The element parameters of (a) coating capacitance, (b) coating resistance, (c) electric double-layer capacitance and (d) charge transfer resistance obtained from fitted EIS of the coatings contained 15 wt% KH550-BS immersed in 3.5 wt% NaCl for different time.



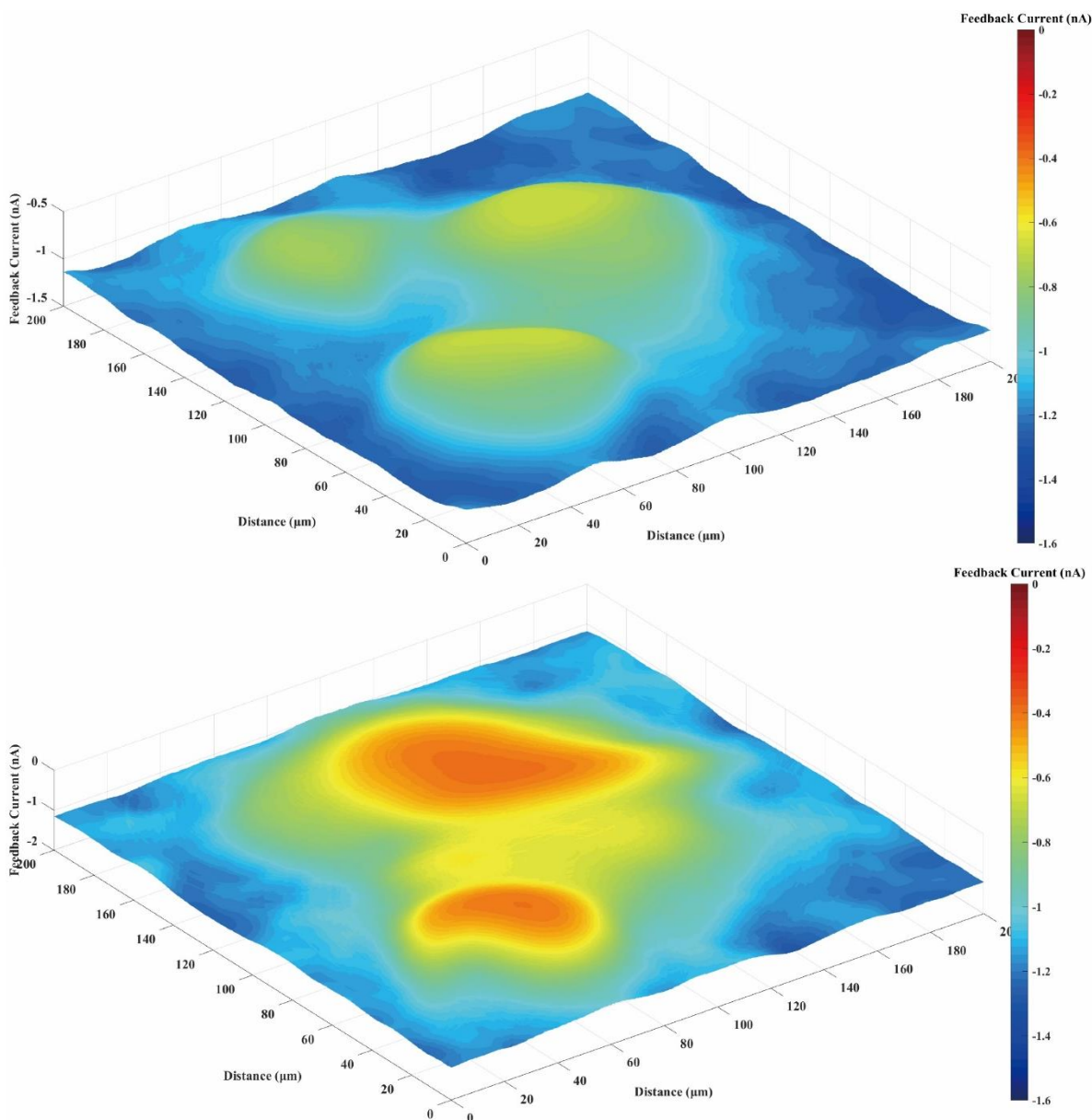


**Figure 10.** Evolution of SECM plots of the sample surface immersed in NaCl solution over time.

### 3.2 Shielding anti-corrosion performance and retarded diffusion dynamics

The better and more stable the basalt scale dispersion effect, the stronger the shielding of the coatings against the penetration of corrosive solution, and the lower the water content in the coatings. Therefore, the dispersion of Basalt scales and the promoting effect of organosilicon on their stable dispersion were investigated and analyzed by the shielding characteristics of the coatings to corrosive solution and the corresponding diffusion kinetics.

The penetration of corrosive electrolyte solution was the leading cause of coating failure. The free volume swelling, activation of polymer-pigment interface, dissolution and loss of additives, and the failure behaviors such as partial peeling and blistering of the coatings were all caused by the infiltration of electrolyte. In this experiment, the purpose of the presence of basalt scales was to form the labyrinth

effect generated by scattered distribution to delay the invasion of corrosive media. Among all the corrosive particles infiltrated, the penetration and diffusion rate of water molecules was the fastest [16]. Chloride ions and dissolved oxygen molecules were carried into the free volume space of the coatings along with the penetration of water. Therefore, the research on the water penetration kinetics of the coatings was the basis and core for theoretical simulation of coating failure behavior. The water penetration kinetics of the coatings was based on the function of coating capacitance and water content [9],

$$v(t) = \frac{\ln \frac{C_c(t)}{C_d}}{\ln \varepsilon_w} \quad (2)$$

Where,  $v$  was the volume ratio of water in coatings,  $C_c$  was coating capacitance, which was the function of time, and  $\varepsilon_w$  was the relative permittivity of water.  $C_d$  was dry coating capacitance, that is, the value of function  $C_c(t)$  at  $t = 0$ . For ideal Fick diffusion, the natural logarithm of coating capacitance was linearly related to the square root of time [11], and the slope was

$$\alpha = \frac{d \ln C_c}{d \sqrt{t}} = \frac{2\sqrt{D}(\ln C_\infty - \ln C_d)}{L\sqrt{\pi}} \quad (3)$$

Where,  $C_\infty$  was the water-saturated coating capacitance.  $D$  was the diffusion coefficient of  $H_2O$  molecules.  $L$  was the coating thickness. However, the complex system structure made the permeation and diffusion behavior of water in coatings significantly deviate from Fick diffusion, presenting extremely complex behavior characteristics of two-stage diffusion, S-shaped diffusion, type II diffusion, or even superposition of multiple diffusions. The coatings prepared in this experiment exhibited a variety of water diffusion characteristics. As shown in figure 11, the coating capacitance curves performed four stages, which were linear Fick diffusion region, un-Fick diffusion region, saturation region and secondary growth region. In the linear Fick diffusion region, coating capacitance raised rapidly, which was attributed to the rapid water seepage process. The un-Fick diffusion region was no longer linear, the increase rate of coating capacitance slowed down, which was the slow water seepage process, and the reason for the increase of coating capacitance included coating swelling and microstructure evolution. The saturation region implied that in this time interval, the water content of the coatings reached saturation and remains stable. The average value of coating capacitance in this region was water-saturated coating capacitance. The secondary growth region commonly meant the coating peeling and the occurrence of blistering. Therefore, it was the sign of coating failure.

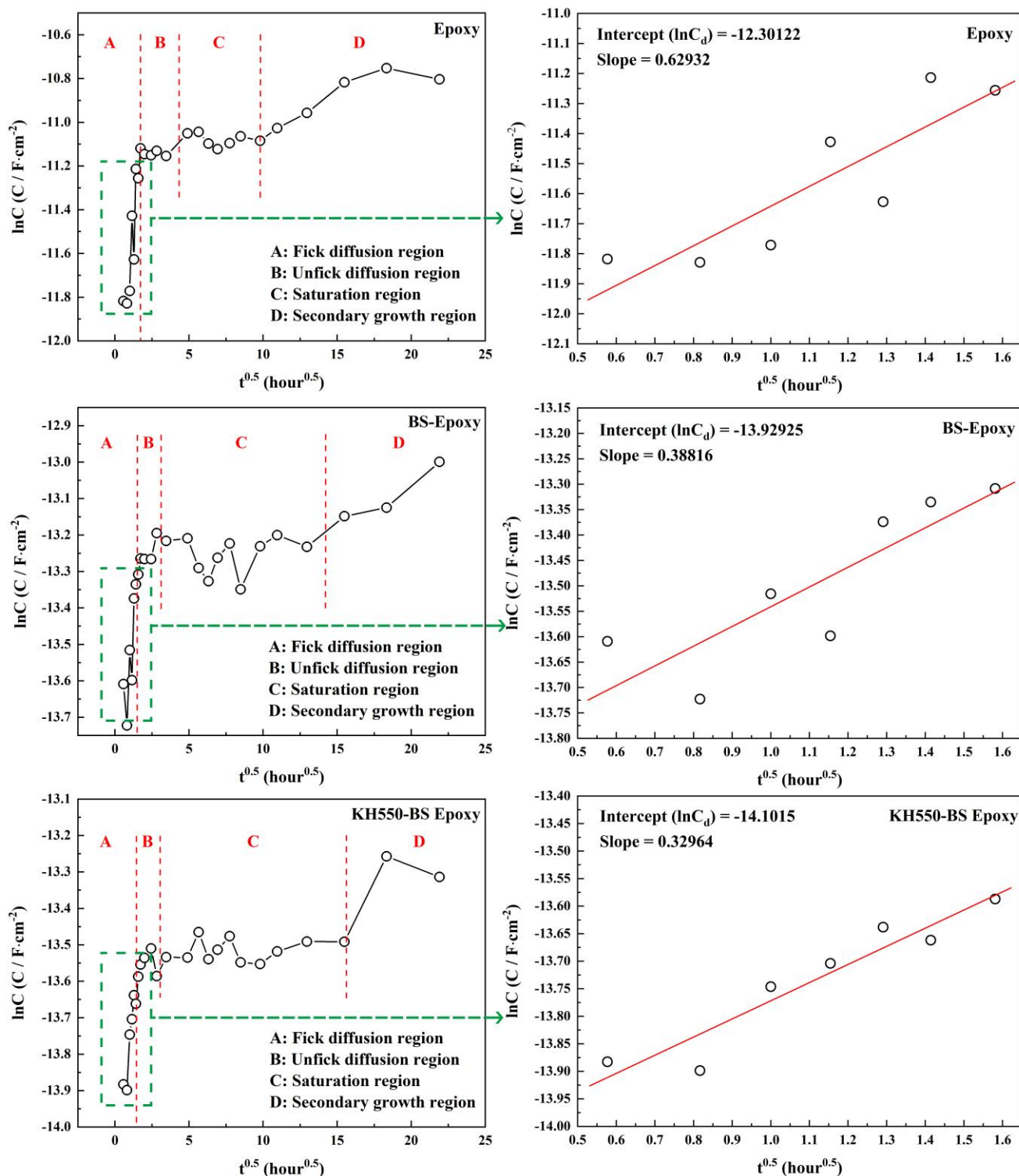


**Figure 11.** The coating capacitance curves of pure epoxy coating, BS-epoxy coating and KH550-BS epoxy coating and the enlarged view of the Fick diffusion region.

Overall, the pure epoxy coating showed the largest coating capacitance. BS and KH550-BS made the coating capacitance move down significantly, and the effect of KH550-BS was the most noteworthy. This indicated that the overall water content of the coatings decreased. Analyzing the linear Fick region

in enlarged view of figure 11 emphatically, BS and KH550-BS eased the slope of straight lines from 0.629 to 0.329, which meant that the water penetration rate was slowed down. KH550-BS performed best. As mentioned earlier, the appearance of secondary growth region marked the beginning of coating failure. The pure epoxy coating failed in about 100 hours ( $t^{0.5} = 10$ ). BS and KH550-BS delayed the expiration time to approximately 196 hours ( $t^{0.5} = 14$ ) and 256 hours ( $t^{0.5} = 16$ ), respectively. In summary, KH550-BS significantly slowed down the water penetration rate in coatings and reduced the water content, thus prolonging the coating life and improving anti-corrosion effects. This was due to the excellent dispersion and its stability of KH550-BS. The nucleophilic addition reaction between  $-NH_2$  of organosilicon and the epoxy groups of epoxy polymer made the BS were fixed by covalent interaction to avoid its settlement and agglomeration as shown in figure 5.

#### 4. CONCLUSION

In this experiment, silane coupling agents KH550 (3-aminopropyl triethoxysilane) and KH560 (3-(2,3-epoxy propoxy) propyltrimethoxysilane) were adopted to modify the basalt scales. The application of modified BS in epoxy coating caused remarkable positive changes in anti-corrosion effects due to the combination of inorganic and organic interfaces and the stable distribution of BS were realized by grafted organosilane. KH560 containing epoxy groups improved the dispersion of basalt scales through the compatibility with epoxy resins rich in epoxy groups. KH550 containing amino groups realized the anchoring of basalt scale in the form of covalent bonds through the ring opening reactions with the epoxy groups of epoxy resin, so as to stabilize the dispersion of basalt scales. KH550-BS behaved the best. Basalt scales and its sheet array acted as the reinforced barrier which slowed down the infiltration of electrolyte solution, reduce the volume ratio of water in the coatings, improved the corrosion protection effect and prolonged the validity of the coatings.

#### ACKNOWLEDGEMENTS

We gratefully acknowledge the support of Shandong Natural Science Foundation, Grand NO. ZR2020QB071, Open Fund supported by Key Laboratory of Marine Materials and Related Technologies, CAS and Zhejiang Key Laboratory of Marine Materials and Protective Technologies, Grand NO. 2021K08, National College Students' innovation and Entrepreneurship Project supported by Ministry of education of the people's Republic of China, Grand NO. 202111066011, Open Fund supported by State Key Laboratory of Marine Coatings (Marine Chemical Research Institute), Graduate Innovation Foundation of Yantai University, Grand NO. YDZD2105, Laboratory Open Fund supported by Yantai University, Grand NO. 003454.

#### References

1. W. Wang, H. Wang, J. Zhao, X. Wang, C. Xiong, L. Song, R. Ding, P. Han and W. Li, *Chem. Eng. J.*, 361 (2019) 792.
2. X. Ji, W. Wang, J. Duan, X. Zhao, L. Wang, Y. Wang, Z. Zhou, W. Li and B. Hou, *Prog. Org. Coat.*,

- 161 (2021) 106454.
3. Archbold, Paul, Tharmarajah and Gobithas, *PCI journal*, 61 (2016) 69.
  4. H.B. A, O.A. B and M.Y.D. C, *Constr. Build. Mater.*, 37 (2012) 629.
  5. M.M. Shokrieh and M. Memar, *App. Compos. Mater.*, 17 (2010) 121.
  6. V.V. Efanova and V.N. Belinskii, *Mech. Compos. Mater.*, 30 (1994) 308.
  7. W. Wang, L. Xu, H. Sun, X. Li, S. Zhao and W. Zhang, *J. Mater. Chem. A*, 3 (2015) 5599.
  8. J. Yan, J. Shi, P. Zhang, W. Tian, Y. Zhang and Z. Sun, *Mater. Corr.*, 69 (2018) 1669.
  9. R. Ding, Y. Zheng, H. Yu, W. Li, X. Wang and T. Gui, *J. Alloy. Compd.*, 748 (2018) 481.
  10. R. Ding, S. Chen, N. Zhou, Y. Zheng, H. Tian, B. Li, X. Wang, T. Gui, W. Li and H. Yu, *J. Alloy. Compd.*, 784 (2019) 756.
  11. R. Ding, W.-w. Cong, J.-m. Jiang and T.-j. Gui, *J. Coat. Tech. Res.*, 13 (2016) 981.
  12. Q.-x. Yue, L.-f. Wu, J. Lv, A.-m. Wang, R. Ding, Y.-y. Wang, L. Yue, W. Gao, X.-l. Li and X.-y. Li, *Colloid Interfac. Sci.*, 45 (2021) 100505.
  13. R. Kalnina, V. Priednieks, K. Lukins, A. Gasparjans and A. Rijkure, *Latv. J. Phys. Tech. Sci.*, 58 (2021) 64.
  14. Qiang, Pei, Wang, Jixiao, Fuyou and Zhi, *Progress in Organic Coatings: An Inter. Rev. J.*, 110 (2017) 1.
  15. G. Chun-tao, The preparation and properties research of epoxy coating modified by basalt flakes, in, Harbin Engineering University, 2016.
  16. R. Ding, J. Jiang and T. Gui, *J. Coat. Tech. Res.*, 13 (2016) 501

© 2022 The Authors. Published by ESG ([www.electrochemsci.org](http://www.electrochemsci.org)). This article is an open access article distributed under the terms and conditions of the Creative Commons Attribution license (<http://creativecommons.org/licenses/by/4.0/>).